Analytical Expressions for the Luminescence of Dilute Quaternary InAs(N,Sb) Semiconductors

C.I. Oriaku[1,2], T. Spencer[1] , X. Yang[3], J. P. Zubelli[3] and M.F. Pereira[1,4]
[1]Materials and Engineering Research Institute, Sheffield Hallam University, S1 1WB, Sheffield, UK, e-mail: m.pereira@shu.ac.uk
[2]Department of Physics Michael Okpara University of Agriculture, P.M.B. 7267, Nigeria
[3]IMPA, Rio de Janeiro, 22460-320, Brazil

Abstract. In this paper, we calculate the luminescence of the dilute quaternary InAs(N,Sb). The theory starts with the band anticrossing model applied to both conduction and the valence band to generate input for analytical approximations that lead to luminescence spectra, including relevant many body effects. Direct application of the equations leads to good agreement with recently measured experimental data.

1. Introduction

One of the most widely studied dilute semiconductors is InAsN [1-4]. Similar to other III-V dilute semiconductors, InAsN exhibits a very large energy band gap bowing which is due to the remarkable variations in the atomic sizes and electronegativity [5] between the nitrogen and InAs. This results in the substitution of a small fraction of the N atoms for InAs and hence the conduction band is perturbed by the N-impurity localized state which is usually below the conduction band edge of InAs. The mechanism of the resulting conduction band edge reduction has been explained by the so called conduction band anticrossing model [9, 14]. A further improvement has been reported [2, 3] on the spectral qualities of InAsN by the introduction of Sb ion. This yields a narrower band gap InNAsSb alloy semiconductor, and has been successfully done using Sb flux in molecular beam epitaxy and a redshift in band gap on the incorporation of Sb has been reported [5]. The band gap engineering by incorporating Sb ion is known to emit at the spectral range between 3 and 5 μm, which is a potential candidate in medical diagnostics and free space communication and atmospheric pollution sensors [6, 7]. Also, strained InAsNSb epilayers on InAs substrate for LED applications have been reported [2]. Just as the presence of the N impurity reduces the

conduction band edge, the incorporation of Sb increases the valence band edge thereby causing a further reduction in the band gap [6]. In fact it has been noted that the roles of Sb in InAsN are to serve as a surfactant [2, 5] and also that when a little amount is incorporated into the lattice it can be used to tune the band gap of InAs(N,Sb) [2]. This paper extends the formalism developed in Ref. [8] and delivers very good agreement between theory and recent experimental data found in the literature.

2. Outline of the mathematical model and material properties

2.1 Bandstructure

The incorporation of Sb in InAsN semiconductor yields an alloy of the form $InAs_{1-x-y}N_xSb_y$. Here x and y are N and Sb mole fractions respectively. In the treatment of the band gap energy of $InAs_{1-x-y}N_xSb_y$ alloy, the band anticrossing model is applied on the conduction band and the valence band since the reduction of the band gap energy is due to the presence of both N and Sb impurities. At the conduction band, N is substituted in small amount for the $As-$atom in the binary InAs introducing an $N-$ isoelectronic level. A similar approach has been applied in the study of GaAsNSb [9]. The solutions of the resulting dispersive eigenstates give doubly degenerate subbands described by the conduction band anticrossing model (BAC)

$$E_{\pm}^{C}(k)=\frac{1}{2}\left[E^{N}+E_{C,InAs}(k)\pm\sqrt{\left[E^{N}-E_{C,InAs}(k)\right]^{2}+4V_{N}{}^{2}x}\right], \qquad (1)$$

Here E^N, $E_{C,InAs}$ and V_N are the N- isoelectric level, conduction band edge energy and the matrix element describing the coupling constant between the N- impurity level and the extended conduction band state. Similarly, in the valence band, the presence of the Sb atom introduces an impurity state below the valence band maximum of $InAs$. This supports the application of the result of a 12 x 12 band **k·p** method [10] for valence band anticrossing model with the subband energy eigenvalues

---

[4] To whom any correspondence should be addressed.

$$E_{\pm}^{hh}(k)=\frac{1}{2}\left[E^{Sb}+H\pm\sqrt{\left[E^{Sb}-H\right]^{2}+4V_{Sb}{}^{2}y}\right], \quad (2)$$

$$E_{\pm}^{lh}(k)=\frac{1}{2}\left[E^{Sb}+L\pm\sqrt{\left[E^{Sb}-L\right]^{2}+4V_{Sb}{}^{2}y}\right], \quad (3)$$

$$E_{\pm}^{SO}(k)=\frac{1}{2}\left[E^{Sb-SO}+S\pm\sqrt{\left[E^{Sb-SO}-S\right]^{2}+4V_{Sb}{}^{2}y}\right], \quad (4)$$

where H and $L,$ denote the valence band energies for the heavy-holes (hh) and light hole lh band respectively band of the binary $InAs$ semiconductor. The spin orbit split-off energy (SO) is denoted by S. Within the 12 x 12 **k·p** band the energies are given as, $H=-\hbar^{2}k^{2}/2m_{hh}+\Delta E_{VBM}\,y$, $L=-\hbar^{2}k^{2}/2m_{lh}+\Delta E_{VBM}\,y$ and $S=(H+L)-\Delta_{0}-\Delta E_{SO}y$ respectively, where Δ_{0}, m_{lh} and m_{hh} are the spin orbit, light-hole and heavy-hole effective masses of $InAs$ semiconductor. The impurity levels of the heavy holes and the spin orbit split-off bands are denoted by E^{Sb} and E^{Sb-SO} respectively. The matrix element for the coupling constant which describes the interaction between Sb and the valence band states is denoted by V_{Sb}. The theoretical value of the band gap of the quaternary $InAs_{1-x-y}N_{x}Sb_{y}$ alloy can thus be obtained taking into account the virtual crystal approximation (VCA), as the difference between the band extrema E^{c} and E^{v}. In this case the band extrema are given as $E^{c}=E_{-}^{c}-\Delta E_{C}$ and $E^{v}=E_{+}^{hh}-\Delta E_{V}$, where ΔE_{C} and ΔE_{V} are the conduction and valence band discontinuities between the end point binaries i.e. $InAs$ and $InSb$. The valence band positions $E_{v,InAs}$ and $E_{v,InSb}$ of the binaries $InAs$ and $InSb$ can be calculated [11] by using $E_{v,InAs}=E_{vav,InAs}+\Delta_{0,InAs}/3$ and $E_{v,InSb}=E_{vav,InSb}+\Delta_{0,InSb}/3$. Their corresponding conduction band positions are $E_{c,InAs}=E_{v,InAs}+E_{g,InAs}$ and $E_{c,InSb}=E_{v,InSb}+E_{g,InSb}$ respectively. The spin orbit split-off energy position are calculated $E_{SO,InAs}=E_{vav,InAs}-2\Delta_{0,InAs}/3$ and $E_{SO,InSb}=E_{vav,InSb}-2\Delta_{0,InSb}/3$. Here E_{vav} and Δ_{0} represent the average valence subband and spin orbit energy of $InAs$ or $InSb$ semiconductor respectively. The conduction, valence and spin orbit split-off band discontinuities between the binaries $InAs$ and $InSb$ are then respectively evaluated as $\Delta E_{C}=E_{c,InAs}-E_{c,InSb}$, $\Delta E_{v}=E_{v,InSb}-E_{v,InAs}$ and $\Delta E_{SO}=E_{SO,InSb}-E_{SO,InAs}$.

2.1 Luminescence

The optical response of semiconductor materials can be obtained by self-consistent evaluation of Many body Nonequilibrium Green's Functions (NEGF), which have been successfully applied to intersubband [12-14] and interband transitions [15-16] in quantum wells and superlattices. This paper starts from an approach that can also describe superlattices as effective 3D anisotropic media [17] and leads to very accurate approximations. Starting from the equation for the interband polarization, an analytical solution for semiconductor luminescence has earlier been derived in Ref. [8] a microscopic approach,

$$L(\omega)=L_0\left[\frac{\hbar\omega}{E_0}\right]^3\frac{1}{e^{\beta(\hbar\omega-\mu)}+1}\left\{\sum_{\ell=1}^{g^{1/2}}\frac{4\pi}{\ell}\left[\frac{1}{\ell^2}-\frac{\ell^2}{g^2}\right]\delta_\Gamma\left(\Delta-\frac{E_\ell}{E_0}\right)+2\pi\int_0^\infty d\phi\frac{\sinh\pi g\sqrt{\phi}}{\cosh\pi g\sqrt{\phi}-\cosh\pi\sqrt{\phi g^2-4g}}\delta_\Gamma(\Delta-\phi)\right\}, \quad (5)$$

where, here $L_0=|\wp|^2E_0^2n_b/\pi^2\hbar^3c^3a_0^3$, $\wp$, n_b, c, E_0 and a_0 are is the dipole matrix element, background refractive index, speed of light in vacuum, exciton binding energy and Bohr radius respectively. ϕ, β and μ are the integration variable, inverse thermal energy and quasiparticle chemical potential with respect to the band gap energy of the dilute nitride material E_g. The probe photon energy $\hbar\omega$ is detuned by $\Delta=\hbar\omega-E_g/E_0$, where E_g is renormalized, following the standard Mott criterion as reported in ref. [17]. The bound state energies are given as $E_l=-E_0\left(l^{-1}-g^{-1}l\right)^2$. The integral runs from ℓ = 1 through the square root of the band state factor g. The optical properties depend largely on the band gap of the quaternary alloy which is influenced by Sb and N mole fractions. In fact, one would expect a much stronger dependence on N mole ratio than Sb mole since it's only a small part of the latter that enters the lattice of the quaternary alloy [4]. The distribution of the N mole fraction x, is expected to cause an inhomogeneous broadening of the photoluminescence spectra of $InAs_{1-x-y}N_xSb_y$ alloy. Here, the inhomogeneously broadened luminescence is approximated as a statistical average of the homogeneously broadened luminescence spectra

$$L_{inh}(\omega)=\int_{-\infty}^{+\infty}L(\omega,x)G(x)dx, \quad (6)$$

Here, $G(x)$ is the Gaussian linewidth having a nominal N- mole fraction x_0 and standard deviation σ_x given by $G(x)=1/\sqrt{2\pi}\sigma_x e^{-\left((x-x_0)/2\sigma_x^2\right)}$. Details of all expressions above are given in Ref. [8]. The goal of this paper is to extend the approach to

quaternary materials and describe corresponding experimental results. In the simulations presented next we just considered a distribution *G(x)* (Nitrogen related) and let y (Sb) as a fixed parameter.

3. Numerical results and discussions

In our calculations, the N impurity level is taken with the form $E^N = E^{N0} - \alpha x$, where the value $E^{N0} = 1.48eV$ [5], instead of the tight binding approximation values of $E^{N0} = 1.36eV$ in Ref. [1], using $\alpha = 2$ from Ref. [1, 5]. The free fitting parameter V_N is taken as $V_N = 2eV$, following Ref. [18]. The position of the Sb level $E^{Sb} = 1.0eV$ [9] the corresponding spin orbit splitting energy impurity level, $E^{Sb-S0} = 1.6eV$ and the free parameter for the valence band $V_{Sb} = 1.05eV$, were used in the calculations [9, 19]. Figure 1 shows the schematic diagram of the band lineup of $InAs_{1-x-y}N_xSb_y$ using the BAC model.

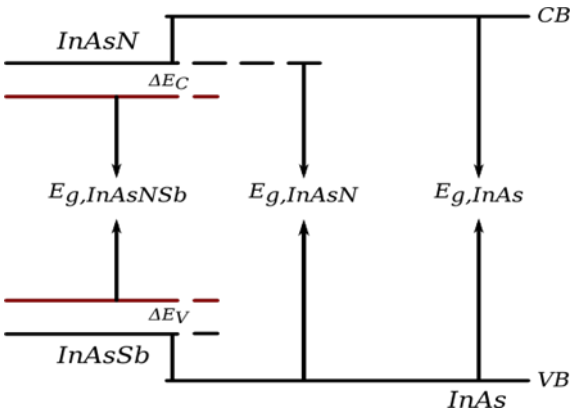

Figure 1. Band schematics of $InAs_{1-x-y}N_xSb_y$ dilute semiconductors.

The conduction band (CB) minimum is controlled by the N-mole fractions and the valence band (VB) maximum is controlled by the Sb- mole fraction. The Virtual crystal approximation is used to introduce the small band offsets ΔE_C and ΔE_V between the constituent $InAs$ and $InSb$. At zero doping level, i.e. $y = 0$ and $x = 0$, the band gap of the semiconductor is simply $E_g, InAs$ as depicted in the diagram above. The material is completely $InAsN$ when the Sb mole fraction is $y = 0$ and the N - mole fraction is increased to a small amount x. In this case the band offsets are zero and the valence band maximum will be that of $InAs$, instead of $InAsSb$ as can be seen in the diagram. A

narrower band gap $InAs_{1-x-y}N_xSb_y$ is obtained when bot Sb and N-impurities are present. Figures 2(a) and 2(b) below depict the band structure of $InAs_{1-x-y}N_xSb_y$ with a lattice temperature of 295 K, calculated for the mole fraction combinations (a) 1.4%N, 4.1%Sb and 1.8%N and 7.3%Sb. The plots show the dispersions as depicted in equations (1) to (3) above. The dotted lines show the dispersions of the host binary semiconductor, while the solid lines show the corresponding dispersions of dilute quaternary semiconductor.

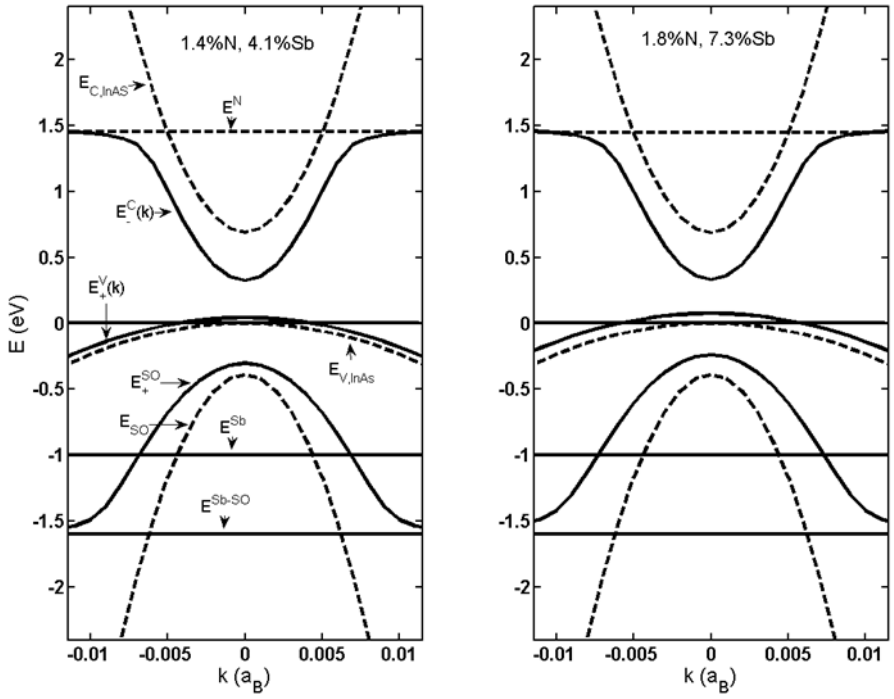

Figure 2. Band structure of $InAs_{1-x-y}N_xSb_y$. (a) 1.4%N, 4.1%Sb and (b) 1.8%N, 7.3% Sb.

Figure 3 compares the computed and experimentally measured luminescence for the different mole fractions. Using the inhomogeneously broadened luminescence given in Eq.6 above, a simple Gaussian distribution with standard deviation $\sigma_x = 0.0025$ was sufficient to obtain a spectrum with a reasonable linewidth. All through the calculations, the density used was $n = 10^{14} carriers/cm^3$. The calculated luminescence spectra are in good agreement with the reported experimental results in Ref. [1].

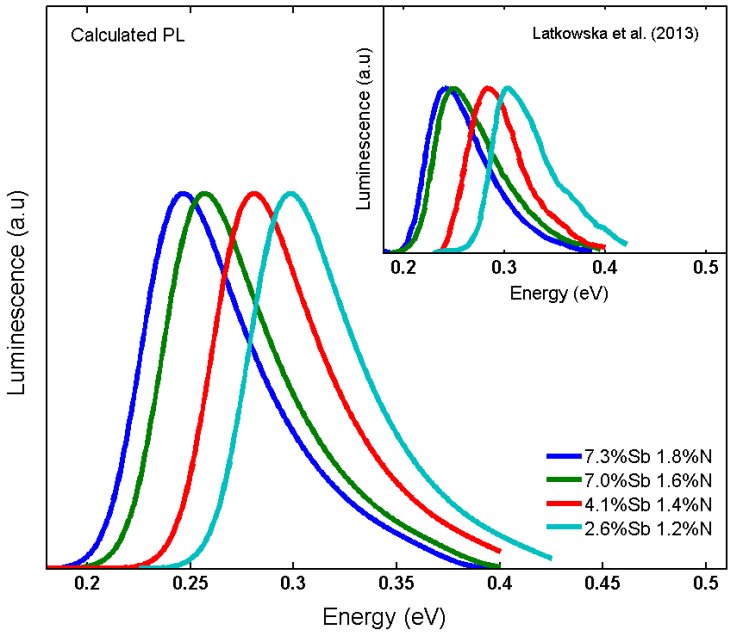

Figure 3. Luminescence of $InAs_{1-x-y}N_xSb_y$ dilute semiconductor. The plots are the calculated luminescence spectra and the inset plots are the measured luminescence extracted from Ref. [1]. The lines are (from left to right) : 1.8%N, 7.3%Sb (blue); 1.6%N, 7.0% Sb (green); 1.4%N, 41% Sb (red); 1.2%N, 2.6% Sb (cyan).

In Figure 4, the luminescence spectra at different carrier temperatures are depicted for two different sample compositions.

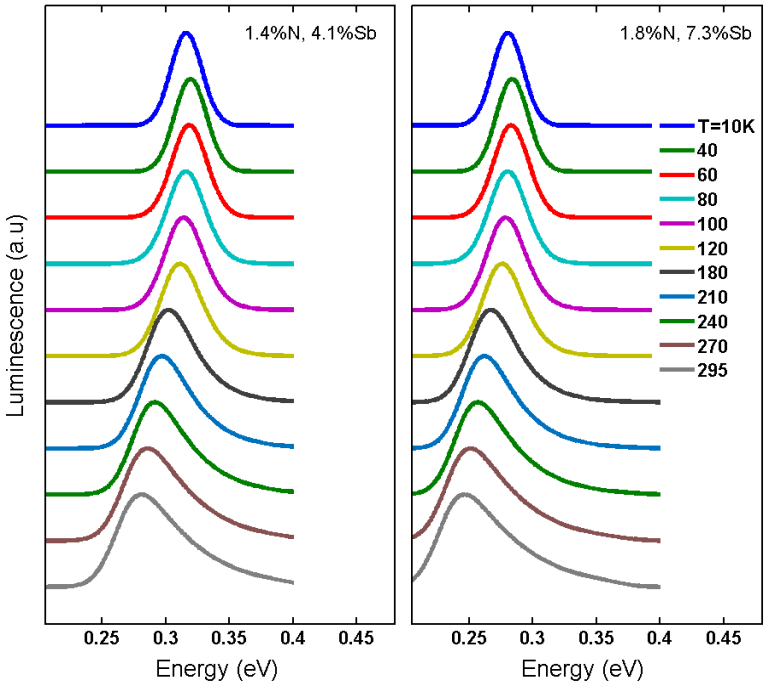

Figure 4. Calculated luminescence of $InAs_{1-x-y}N_xSb_y$. (a) 1.4%N, 4.1%Sb and (b) 1.8%N, 7.3% for different temperatures increasing from 10 K to 295K.

The dependence of the free carrier energy band gaps with temperature are given by the Varshni relation for the host binary material $InAs$ given in Ref. [20], $E_g = E_{g0} - \alpha_0 T^2/T + \beta_0$, where E_{g0} is the low temperature band gap of binary $InAs$ $E_{g0} = 417meV$, α_0 and β_0 are the Varshni parameters given by $\alpha_0 = 0.76meV/K$, $\beta_0 = 93K$. A close look at the plots for the carrier temperatures 10-80K suggests a deviation from the Varshni relation. This is consistent and show similar features with the curves reported in Ref. [1] and is shown in more detail in Figure 5.

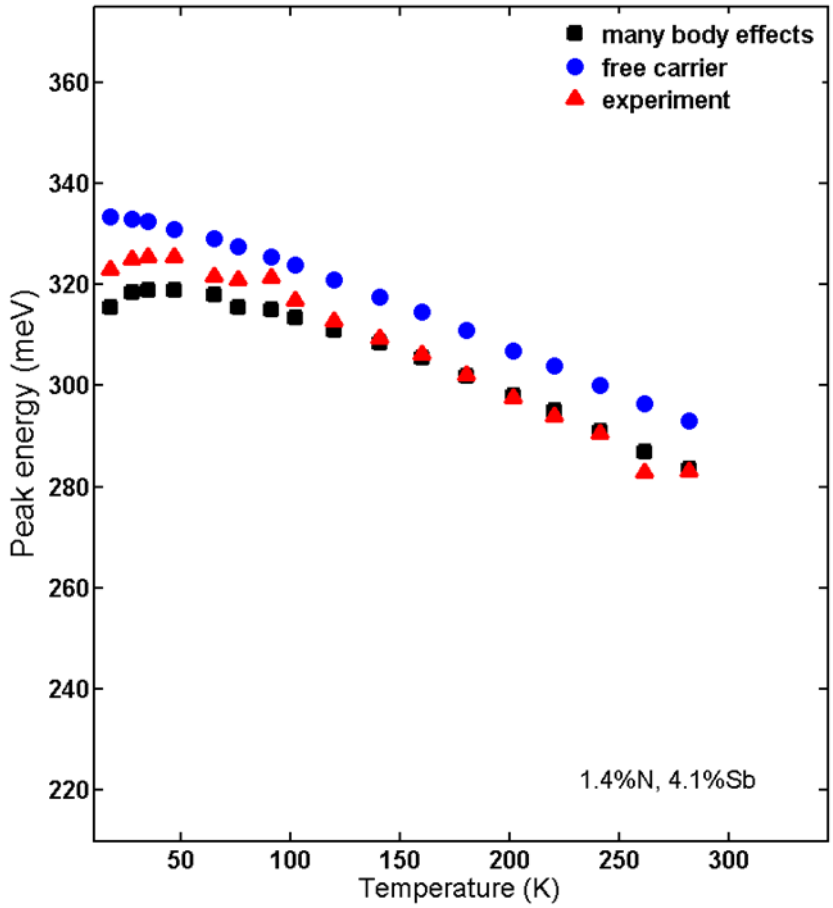

Figure 5. Temperature dependence of the peak luminescence of for the mole fractions 1.4%N, 4.1%Sb. The black square is calculated with our full many body approach, blue circle is the free carrier and the red triangle is the experimental data extracted from Ref. [1] for comparison.

In Figure 5, we present the luminescence energy peaks of $InAs_{1-x-y}N_xSb_y$ with respect to temperature. The calculated emission peaks (black circles) with our full microscopic approach containing the many body effect are in good agreement with the

experimentally measured luminescence energy emission peaks (red triangle) [1]. The blue circles in Fig. 5 depict the free carrier luminescence at different temperatures which dominate the entire spectrum when the bound state factor $g \to 0$. For both the calculated and experimentally observed luminescence, a blue shift is initially observed at low temperatures ~10-80K before a gradual redshift at higher temperatures. The low temperature blue shift is due to exciton ionization, showing clearly the importance of our approach.

4. Conclusion

We have presented in this paper theoretical calculations of luminescence emission in dilute quaternary semiconductors of type $InAs_{1-x-y}N_xSb_y$ The bandstructure was obtained by applying the conduction and valence band anticrossing model on the nitrogen modified conduction band and the Sb modified valence band. The most relevant many body effects were included in our efficient analytical approximations and are necessary to explain the evolution of experimental data with temperature. The results of our calculations show good agreement with recent experimentally observed results.

Acknowledgements

The authors acknowledge support from MPNS COST ACTION MP1204 - TERA-MIR Radiation: Materials, Generation, Detection and Applications and COST ACTION BM1205 European Network for Skin Cancer Detection using Laser Imaging. C.I.Oriaku's research is supported by TETFUND, Nigeria.

References

[1] Latkowska M, Kudrawiec R, Janiak F, Motyka M, Misiewicz J, Zhuang Q, Krier A and Walukiewicz W 2013 Appl. Phys. Lett. 102 122109.

[2] Zhuang Q, Godenir A, Krier A, Tsai G, and Lin H H 2008 Appl. Phy. Let. 93 121903.

[3] Kudrawiec R, Latkowska M, Misiewicz J, Zhuang Q, Godenir A M R and Krier A, 2011 Appl Phys Lett 99 011904.

[4] Chen R, Phann S, Sun H D, Zhuang Q, Godenir A M R and Krier A 2009 Appl Phys Lett 95 261905.

[5] Veal TD, Piper L F J, Jefferson P H, Mahboob I and McConvilleb C F, Merrick M, Hosea T J C, Murdin B N and Hopkinson M 2005 Appl. Phys. Let 87 182114.

[6] Pereira M F, 2014 Opt Quant Electron 46 491.

[7] Pereira M F, 2015 Opt Quant Electron 47 815.

[8] Oriaku C I and Pereira M F, "Analytical solutions for semiconductor luminescence including Coulomb correlations with applications to dilute bismides", Editorially Accepted for Publication at J Opt Soc Am B (Manuscript #278879, 2016).

[9] Lin Y-T, Ma T-C, Chen T-Y and Lin H H 2008 Appl. Phys. Let. 93, 171914.

[10] Alberi K, Wu J, W. Walukiewicz, Yu K M, Dubon O D, Watkins S P, Wang C X, Liu X, Cho Y-J, and Furdyna J (2007) Phys. Rev. B 75 045203.

[11] Chuang S L, Physics of Photonic Devices, 2nd ed., John Wiley & Sons, New York (1995).

[12] Pereira M F 2011J Opt Soc Am B 28 2014.

[13] Pereira M F and Faragai I A 2014 Optics Express 22, 3439.

[14] Pereira M F 2016 Appl. Phys. Lett. 109, 222102.

[15] Pereira Jr M F, Binder R and Koch S W 1994 Appl. Phys. Lett. 64 279.

[16] Grempel H et al 1996 physica status solidi (b) 194 199.

[17] Pereira Jr M F 1995 Phys Rev B 52 1978.

[18] Vurgaftman I and Meyer J R, 2003 Journal of Applied Physics 94 3675.

[19] Aissat A, Nacer S, Seghilani M, Vilcot J P 2010 Physica E 43 40–44.

[20] Vurgaftman I, Meyer J R, and Ram-Mohan L R 2001 Journal of Applied Physics 89 5815.